Transmission Defense Hardening Against Typhoon Disasters Under Decision-Dependent Uncertainty

Weixin Zhang, Changzheng Shao, *Member, IEEE*, Bo Hu, *Member, IEEE*, Kaigui Xie, *Senior Member, IEEE*, Pierluigi Siano, *Senior Member, IEEE*, Mushui Li, and Maosen Cao

***Abstract*—Transmission defense hardening (TDH) is an effective practice to ensure the safe operation of the power system during and after natural disasters, such as typhoons. However, the coupling among the typhoon disaster, hardening decision, and transmission line status is not addressed in the previous research works. Besides, the enhancement measures for different types of transmission line failures have not yet been assessed. This paper proposes a comprehensive framework to improve power transmission system resilience against typhoon disasters. Firstly, the motion path and the wind field of typhoons are simulated using Monte Carlo sampling to quantify the spatiotemporal impacts of wind speed on the transmission line status. The decision-dependent uncertainty (DDU), which reflects the effects of hardening decisions on the transmission lines, is addressed by sampling according to the corresponding failure probabilities. Then, the scenario simulation is integrated into the proposed two-stage stochastic mixed-integer programming (SMIP) model considering various enhancement measures for different failures. Since the way to handle the DDU needs a large number of scenarios, it leads to high computation complexity. Hence, the sample average approximation (SAA) algorithm is introduced to cope with it. Finally, the proposed framework and its solution algorithm are carried out on the modified IEEE RTS-79 system and the modified IEEE 118-Bus system. The significant cost saving and resilience improvement demonstrate the effectiveness of the proposed framework.**

***Index Terms*—Decision-dependent uncertainty, transmission defense hardening, typhoon disasters, sample average approximation, stochastic programming.**

NOMENCLATURE

Abbreviations

TDH	Transmission defense hardening.
SMIP	Stochastic mixed-integer programming.
DDU	Decision-dependent uncertainty.
SAA	Sample average approximation.
DAD	Defender-attacker-defender.
TD	Tower damage.
WYF	Windage yaw flashover.
CI	Confidence interval.

Indices

t	Index of timestamps from 1 to $\|T\|$.
s	Index of scenarios from 1 to $\|S\|$.
g	Index of generation units from 1 to $\|G\|$.
d	Index of loads from 1 to $\|D\|$.
l	Index of transmission lines from 1 to $\|L\|$.

Sets

L	Set of transmission lines.
S	Set of scenarios.
T	Set of timestamps.
A	Set of enhancement measures against TD.
B	Set of enhancement measures against WYF.
G	Set of generation units.
G_b	Set of generation units connected to bus b.
LF_b	Set of lines flow from bus b.
LT_b	Set of lines flow to bus b.
D	Set of loads.
D_b	Set of load connected to bus b.

Parameters

c_l^a	Enhancement cost for taking enhancement measure a against tower damages on line l.
c_l^b	Enhancement cost for taking enhancement measure b against windage yaw flashovers on line l.
c^R	Cost for repairing one transmission line.
c_d	Penalty cost for shedding 1 MWh load.
ω	Average number of typhoon attacks in a year.
$\mathbb{E}_s$	An operation that denotes a mathematical expectation.
N_L	Maximum number of enhancement measures that can be taken.
π^s	Occurrence probability of typhoon scenario s.
$\xi_{l,t}^{0,s}$	Parameter representing the damage status of line l if it is not hardened, damaged (1) or normal (0) at timestamp t in scenario s. (Caused by TD).

Manuscript received 20 December 2021; revised 16 May 2022; accepted 24 July 2022. Date of publication 27 July 2022; date of current version 24 April 2023. This work was supported by the National Natural Science Foundation of China under Grant 52022016. Paper no. TPWRS-01947-2021. *(Corresponding author: Bo Hu.)*

Weixin Zhang, Changzheng Shao, Bo Hu, Kaigui Xie, and Maosen Cao are with the State Key Laboratory of Power Transmission Equipment and System Security, Chongqing University, Chongqing 400044, China (e-mail: weixinzhang@cqu.edu.cn; cshao@cqu.edu.cn; hboy8361@163.com; kaiguixie@vip.163.com; cms517499119@outlook.com).

Pierluigi Siano is with the Department of Management and Innovation Systems, University of Salerno, 84084 Fisciano, Italy, and also with the Department of Electrical and Electronic Engineering Science, University of Johannesburg, 2006 Johannesburg, South Africa (e-mail: psiano@unisa.it).

Mushui Li is with the State Grid Chongqing Changshou Electric Power Supply Branch, 401220 Chongqing, China (e-mail: 934910580@qq.com).

Color versions of one or more figures in this article are available at https://doi.org/10.1109/TPWRS.2022.3194307.

Digital Object Identifier 10.1109/TPWRS.2022.3194307

0885-8950 © 2022 IEEE. Personal use is permitted, but republication/redistribution requires IEEE permission.
See https://www.ieee.org/publications/rights/index.html for more information.

Authorized licensed use limited to: b-on: Universidade de Coimbra. Downloaded on November 09,2024 at 17:13:41 UTC from IEEE Xplore. Restrictions apply.

$\xi_{l,t}^{a,s}$ Parameter representing the damage status of line l if it is hardened through measure a, damaged (1) or normal (0) at timestamp t in scenario s. (Caused by TD).

$\gamma_{l,t}^{0,s}$ Parameter representing the damage status of line l if it is not hardened, damaged (1) or normal (0) at timestamp t in scenario s. (Caused by WYF).

$\gamma_{l,t}^{b,s}$ Parameter representing the damage status of line l if it is hardened through measure b, damaged (1) or normal (0) at timestamp t in scenario s. (Caused by WYF).

$P_g^{\max}$ Upper limit of the active power output of generation unit g.

$P_{d,t}$ Load demand d at timestamp t.

$\theta_b^{\min}/\theta_b^{\max}$ Minimum / Maximum phase angle of bus b.

$P_l^{\max}$ Maximum capacity of line l.

M_c A large constant.

b_l Susceptance of line l.

Variables

C^E Total enhancement cost of line hardening.

$C^{R,s}$ Total repair cost in scenario s.

$C^{L,s}$ Total penalty cost for load shedding in scenario s.

$\phi(s)$ Total penalty costs for load shedding and repair in scenario s.

x_l^{tower} Binary variable representing whether line l is hardened against TD (1) or not (0).

$x_l^{flashover}$ Binary variable representing whether line l is hardened against WYF (1) or not (0).

$x_l^{a,T}$ Binary variable representing whether line l is hardened against TD through measure a (1) or not (0).

$x_l^{b,F}$ Binary variable representing whether line l is hardened against WYF through measure b (1) or not (0).

$u_{l,t}^s$ Binary variable representing line l is damaged (1) or not (0) at timestamp t in scenarios s. (Caused by TD).

$v_{l,t}^s$ Binary variable representing line l is damaged (1) or not (0). at timestamp t in scenarios s (Caused by WYF).

$y_{l,t}^s$ Binary variable representing line l is damaged (1) or not (0) at timestamp t in scenarios s.

$P_{g,t}^s$ Active power output of generation unit g at timestamp t in scenario s.

$\tilde{P}_{d,t}^s$ Load shedding of load d at timestamp t in scenario s.

$\theta_{b,t}^s$ Phase angle of bus b at timestamp t in scenario s.

$P_{l,t}^s$ Power flow of line l at timestamp t in scenario s.

$\theta_{l,fr,t}^s$ Phase angle of the beginning of line l at timestamp t in scenario s.

$\theta_{l,to,t}^s$ Phase angle of the end of line l at timestamp t in scenario s.

$w_{l,t,1}^s$ Binary auxiliary variable.

$w_{l,t,2}^s$ Binary auxiliary variable.

I. Introduction

TYPHOON, also called hurricane [1], is one of the severest natural disasters that threaten the regular operation of the power system. For example, Typhoon Sandy hit the northeast region of the United States, causing power outages for millions of users in December 2012 [2]. In 2016, Typhoon Meranti destroyed the power grid in Fujian, China. Millions of electrical users were affected, and the direct economic loss was as high as 21 billion RMB [3]. To reduce or eliminate the related risks, pre-disaster defense planning has attracted the attention of system planners and researchers. It is an effective way to enhance the power grid to withstand natural disasters.

Previous research works along with optimization algorithms focused on two main thrusts in the process of the pre-disaster transmission defense planning:1) transmission (and generation) defense expansion [4], and 2) transmission defense hardening (TDH) [5]. The former boosts the transmission system resilience through redundant transmission routes. The latter enhances the components to increase the power system performance with stronger, more robust materials or auxiliary assemblies [6].

One of the most commonly used mathematical models for pre-disaster defense planning is the classical tri-level defender-attacker-defender (DAD) framework initially proposed in [7]. In the first level, the defender makes hardening decisions before attacks. In the second level, the attacker destroys the weak part of the system, causing the worst consequences. In the third level, the defender takes corrective actions to minimize the loss. Subsequently, the DAD framework was applied to power system hardening [8] and capacity expansion and switch installation [9]. However, the classical DAD framework is initially proposed to address the worst-case situation under various attacks. It cannot distinguish the failure probabilities of individual components. Additionally, the classical DAD framework assumes that the hardened components will be never damaged in future attacks, which is not practical in engineering.

Some research works attempted to address these issues by constructing or modifying uncertainty sets. Reference [10] designed a multi-stage multi-zone uncertainty set to capture the spatial-temporal dynamics of extreme weather events. In [11], the distributionally robust optimization theory was applied to the DAD framework. The component survivability, post-disaster system failure state, and historical data are utilized to construct the confidence sets for their ambiguous probability distributions. The uncertainty set was modified in [12] based on Claude Shannon's information theory. The uncertainty budget of the component with lower failure probability is larger, which can differentiate the effects of enhancement measures to some extent. Whereas, the uncertainty of extreme weather events is still not fully addressed in these improved DAD frameworks. Besides, the results are usually over-conservatism and strongly reliant on uncertainty budgets.

Since natural disasters damage the power systems randomly, a satisfactory pre-disaster defense planning decision will be achieved by a stochastic approach, which can capture the random nature of extreme weather events. Generally, the stochastic

Authorized licensed use limited to: b-on: Universidade de Coimbra. Downloaded on November 09,2024 at 17:13:41 UTC from IEEE Xplore. Restrictions apply.

approaches can be divided into two categories, namely, scenario-based simulation and scenario-based optimization.

Scenario-based simulation mainly focuses on assessing power system resilience. A sequential Monte Carlo-based simulation model was introduced to evaluate the effects of extreme weather events and various enhancement measures on power system resilience [13]. Reference [14] proposed a stochastic framework for the resilience assessment of weather-coupled and repairable power systems. In [15], a resilience assessment framework was proposed to identify the vulnerable parts of the transmission system. Then, the power system resilience was improved by hardening the weakest corridor or increasing redundancy to meet the desired level. Nevertheless, simulation methods can usually assess the impact of different enhancement measures on power systems based on the proposed resilience metrics but cannot be efficiently utilized to determine an optimal enhancement portfolio.

The optimal planning decision that minimizes the expected cost of all scenarios can be obtained using scenario-based optimization. Usually, the clustering technique [16] and scenario reduction technique [17] are utilized to reduce the computational complexity. In [18], a two-stage stochastic optimization model was established for transmission and generation expansion to mitigate the risk caused by earthquakes considering six typical scenarios. In [19], a scenario reduction approach is utilized to construct representative substation failure scenarios for electrical substations' protection against flood hazards. References [20] and [21] discussed transmission and distribution system resilience enhancement, respectively. The hardened lines are assumed to become invulnerable to extreme weather events [20]. Instead, a more reasonable assumption was made in [21]. It supposes that the damage probability will be reduced due to the hardening but not be reduced to zero. The uncertainty of the parameters faced later that will be influenced by decisions is called decision-dependent uncertainty (DDU) or endogenous uncertainty [22]. The DDU was handled by sampling to decouple the interrelation between hardening decisions and line status. However, the vulnerability of the distribution line is determined without fully considering the random nature of the typhoon disasters.

Indeed, there exists a coupling among the typhoon disasters, hardening decisions, and transmission line status. On the one hand, the risk of line damage is influenced by the intensity of the typhoon disasters. Usually, the transmission system is spatially distributed, leading to different transmission lines and even different sections of the same transmission line are affected dissimilarly during the movement of the same typhoon. Hence, it is necessary to simulate the typhoon motion path and the wind field to obtain the spatiotemporal impacts of wind speed on the transmission line status. On the other hand, hardening decisions will improve the transmission lines' resistance to various typhoon disasters to varying degrees. Thus, the transmission line failure probabilities should be also modeled by linking the uncertainty description to the line hardening. Since the transmission line status is simultaneously influenced by both the severity of the typhoon and the decisions related to the TDH, a more satisfactory hardening decision will be made after well addressing the coupling.

Besides, according to the report of the State Grid Typhoon Monitoring & Warning Center [23], the transmission line damages are mainly caused by tower damages (TD) and wind-age yaw flashovers (WYF) during typhoon disasters, which account for 44.8% and 41.3%, respectively. The remaining 13.9% includes ground wire disconnection, foreign matter, etc. Therefore, the individualized enhancement measures for different types of failures should be considered. Additionally, there are usually several ways to suppress the failure probability. For example, the strength of the transmission tower can be enhanced by adding a series of diaphragm bracing types at the mid-height of the slender diagonal members [24] or attaching additional parallel angle members to retrofit steel angles [25]. The probability of WYF can be reduced by using rigid jumpers or using windproof insulators [26]. Obviously, the costs and effects of different enhancement measures are different. It is best to implement different enhancement measures for different transmission lines based on their vulnerability and their importance to the system. However, only a single line hardening measure was considered in the previous research works [15], [21].

To overcome these challenges, this paper proposes a comprehensive framework for TDH against typhoon disasters with consideration of the DDU. The proposed framework can help planners make a better hardening decision. In this framework, ignoring differences in factors such as terrain, we first generate the typhoon disaster scenarios, including motion path [27] and wind field [28]. Further, we assume that the lines will only be outage due to TD and WYF. It is assumed that the planner has prior knowledge of the failure probabilities of transmission lines with or without enhancement measures. Practically, the wind resistance of transmission lines can be estimated by means such as finite element analysis. Thereby, the status of transmission lines can be determined in each specific typhoon disaster. The DDU that reflects the effects of hardening decisions on transmission lines is handled by the means proposed in [21]. Notably, since the DDU is not described analytically, it needs many scenarios to obtain a high-quality decision. To speed up the calculation, the progressive hedging algorithm was introduced to solve the proposed large-scale two-stage stochastic mixed-integer programming (SMIP) in parallel. Nevertheless, in this way, the optimality of obtained solution can be guaranteed in the sampled scenarios but may not satisfy global optimality. Consequently, in our work, the sample average approximation (SAA) algorithm [29]–[31] is employed to solve the proposed optimization problem. Finally, in this way, the near-optimal resilience enhancement portfolio and confidence interval (CI) of the optimal value can be derived.

The main novel contributions of our work are listed as follows:

1) The coupling among typhoon disasters, hardening decisions, and transmission line status is addressed. The interrelation between typhoon disasters and transmission line status is handled by quantifying the spatiotemporal impacts of various typhoon disasters on the transmission lines. The interdependency between the hardening

Authorized licensed use limited to: b-on: Universidade de Coimbra. Downloaded on November 09,2024 at 17:13:41 UTC from IEEE Xplore. Restrictions apply.

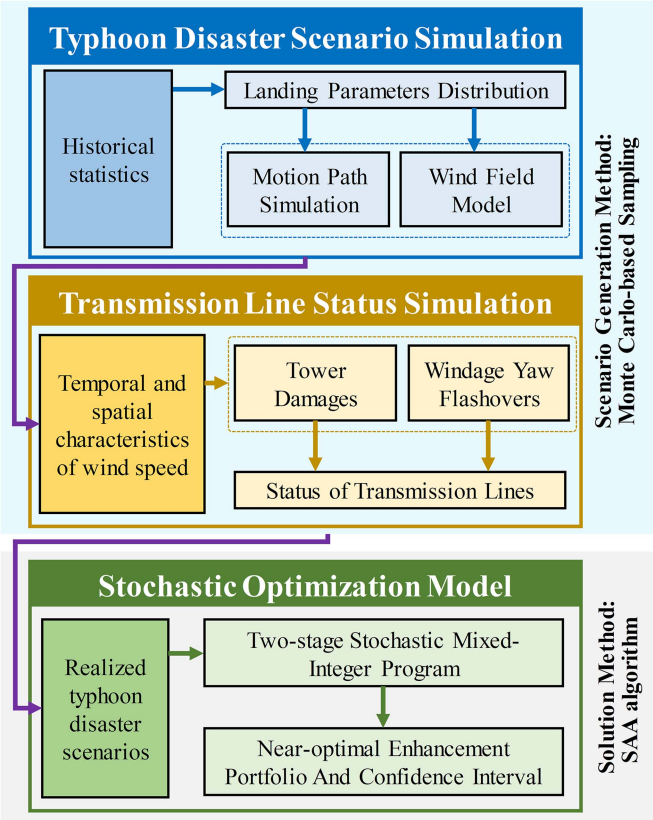

Fig. 1. The proposed TDH framework.

decisions and transmission line status is decoupled by sampling according to the corresponding failure probabilities. This allows us to construct a series of reasonable scenarios for the TDH problem.

2) A two-stage stochastic optimization model is formulated to deal with the TDH problem accounting for different failures. Additionally, enhancement measures for different failures are considered in the optimization model. Therefore, the proposed framework can obtain a more practical hardening decision.

3) The SAA algorithm is introduced to cope with the troublesome decision-dependent structure existing in the proposed optimization model. The SAA algorithm relies on statistical sampling to approximate the underlying stochastic optimization model. It can be utilized to obtain a near-optimal solution and CI of the true optimal value.

The remainder of this paper is organized as follows. Section II introduces the proposed TDH framework. Section III introduces the solution algorithm. The results and analysis for the modified IEEE RTS-79 system and the modified IEEE 118-Bus system are discussed in Section IV. Section V concludes the paper.

II. Proposed Transmission Defense Hardening Framework Against Typhoon Disasters

The proposed comprehensive TDH framework is shown in Fig. 1. It consists of three main modules: 1) a typhoon disaster scenario simulation to simulate various typhoons, 2) a transmission line status simulation to characterize the failure probability associated with wind speed, and 3) a stochastic optimization model that integrates the scenario generation method considering the first two modules to obtain the near-optimal resilience enhancement portfolio.

A. Typhoon Disaster Scenario Simulation

Typhoon disaster scenario simulation mainly consists of two parts, i.e., typhoon motion path simulation, and typhoon wind field simulation. After landing, the typhoon motion path and the wind field can be approximately simulated corresponding to the typhoon landing parameters.

1) The Distributions of the Typhoon Landing Parameters: The typhoon landing parameters, including the moving direction angle, moving speed, and central pressure difference, describe the motion state of the typhoon at the time of landing. In the previous work [32]–[35], the probability distributions of the typhoon landing parameters have been discussed.

The moving direction angle obeys the bi-normal distribution [32], [33], given as follows:

$$f(\theta(0)) = \begin{cases} \frac{1}{\sqrt{2\pi}} \frac{2}{\sigma_1+\sigma_2} \exp\left(-\frac{1}{2}\frac{(\theta(0)-\mu_\theta)^2}{\sigma_1^2}\right), \theta(0) \le \mu_\theta \\ \frac{1}{\sqrt{2\pi}} \frac{2}{\sigma_1+\sigma_2} \exp\left(-\frac{1}{2}\frac{(\theta(0)-\mu_\theta)^2}{\sigma_2^2}\right), \theta(0) > \mu_\theta \end{cases} \tag{1}$$

where μ_θ is the mean of bi-normal distribution; σ_1 and σ_2 are the standard deviations of the two normal distributions, respectively.

The moving speed subjects to the log-normal distribution [34], presented as follows:

$$g(c(0)) = \frac{1}{c(0)\sqrt{2\pi}\sigma_{\ln c}} \exp\left[-\frac{1}{2}\left(\frac{\ln c(0) - \mu_{\ln c}}{\sigma_{\ln c}}\right)^2\right] \tag{2}$$

where $\mu_{\ln c}$ and $\sigma_{\ln c}$ are the mean and standard deviation of the normal distribution corresponding to the log-normal distribution, respectively.

The central pressure difference shares the same Weibull probability density function [35], shown as follows:

$$h(\Delta P(0)) = \frac{\kappa}{\chi}\left(\frac{\Delta P(0)}{\chi}\right)^{\kappa-1} \exp\left[-\left(\frac{\Delta P(0)}{\chi}\right)^{\kappa}\right] \tag{3}$$

where κ and χ are the shape parameter and the scale parameter of the Weibull distribution, respectively.

2) Typhoon Motion Path Simulation: The empirical track model is one of the most mature models to simulate the typhoon motion path [27]. According to the storm track model, the moving speed and moving direction angle in the time stamp $t+1$ can be derived through longitude, latitude, moving speed, and moving direction angle in the current timestamp t and previous timestamp $t-1$.

$$\Delta \ln c(t+1) = a_1 + a_2\psi(t) + a_3\lambda(t) + a_4 \ln c(t) + a_5\theta(t) \tag{4}$$

$$\Delta\theta(t+1) = b_1 + b_2\psi(t) + b_3\lambda(t) + b_4 c(t) + b_5\theta(t) + b_6\theta(t-1) \tag{5}$$

Authorized licensed use limited to: b-on: Universidade de Coimbra. Downloaded on November 09,2024 at 17:13:41 UTC from IEEE Xplore. Restrictions apply.

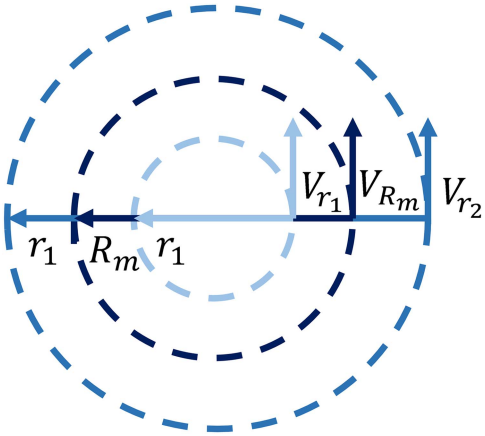

Fig. 2. The typhoon wind field based on the Batts model.

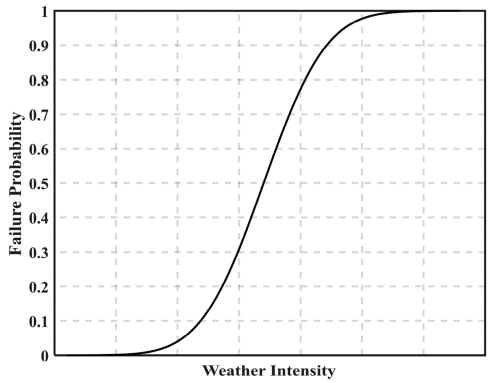

Fig. 3. Generic fragility curve of components in extreme weather.

$$c(t+1) = c(t)\exp\left[\Delta \ln c(t+1)\right] \tag{6}$$

$$\theta(t+1) = \theta(t) + \Delta\theta(t+1) \tag{7}$$

where $c(t)$ represents the moving speed (m/s) of the typhoon at timestamp t; $\theta(t)$ represents the moving direction angle (rad) of the typhoon at timestamp t; $a_1, \ldots, a_5$ and $b_1, \ldots, b_6$ are the constants of the empirical track model, can be determined by fitting historical data; $\psi(t)$ and $\lambda(t)$ are the longitude and latitude of the position of the typhoon center at timestamp t.

Note that the latitude and longitude coordinates and the rectangular coordinates can be converted to each other. Referring to equations (4)-(7), the typhoon motion path can be simulated from the time of landing to the time of disappearance with the initial typhoon landing parameters.

3) Typhoon Wind Field Simulation: The Batts model [28], one of the most developed models, is employed to describe the typhoon wind field. To illustrate it specifically, the typhoon wind field established through the Batts model is presented in Fig. 2. The typhoon wind field is assumed as an axisymmetric circular vortex. The isobars and isotherms of the typhoon are regarded as approximately concentric circles. The wind direction is defined as a counterclockwise tangent.

Further, the wind speed can be calculated as follows:

$$V_r(t) = \begin{cases} V_{R_m}(t)\cdot[r/R_{\mathrm{m}}(t)], & r \le R_{\mathrm{m}}(t) \\ V_{R_m}(t)\cdot[R_{\mathrm{m}}(t)/r]^{\eta}, & r > R_{\mathrm{m}}(t) \end{cases} \tag{8}$$

$$V_{R_{\mathrm{m}}}(t) = 0.865V_{gx}(t) + 0.5c(t) \tag{9}$$

$$V_{gx}(t) = K\sqrt{\Delta P(t)} - [R_{\mathrm{m}}(t)/2]\cdot f \tag{10}$$

$$R_{\mathrm{m}}(t) = \exp\left[-0.1239\Delta P(t)^{0.6003} + 5.1034\right] \tag{11}$$

where $V_r(t)$ represents the wind speed (m/s) of any point in the typhoon wind field at timestamp t; $V_{R_m}(t)$ represents the maximum speed (m/s) of the typhoon wind field aat timestamp t; $R_m(t)$ represents the maximum speed radius of the typhoon wind field at timestamp t; η is a constant with the value between 0.5 and 0.7; $V_{gx}(t)$ means the maximum gradient wind speed (m/s) aat timestamp t; K is a constant equal to 6.72; f is the Coriolis force parameter of the Earth's rotation.

Note that the maximum wind speed calculation is based on the assumption that the typhoon is at the ocean surface all the time. A reduction factor is introduced since the wind speed of the typhoon will attenuate caused by friction after landing. It is defined as follows [28]:

$$\frac{V_{R_m}^{L}(t)}{V_{R_m}^{W}(t)} = \frac{1}{0.2p\ln{}^{10}/_{z_0}} \tag{12}$$

where $p = 0.85$ represents the retardation factor; $z_0 = 0.005$ m represents the roughness length; the superscripts L and W represent "overland" and "overwater", respectively. Hence, $V_{R_m}^{L}(t)/V_{R_m}^{W}(t) = 0.774$.

The central pressure difference will decrease with time after landing. It is given as [28]

$$\Delta P(t) = \Delta P(0) - 0.02(1+\sin\delta)\Delta T_{0,t} \tag{13}$$

where $\Delta P(t)$ represents the central pressure difference (hpa) of the typhoon at timestamp t; δ is the angle between the moving direction and the coastline; $\Delta T_{0,t}$ is the difference between the current timestamp t and the time of the typhoon landing.

According to equations (8)-(13), the wind speed at any point in the wind field can be derived in any timestamp.

B. Transmission Line Status Simulation

There are two main ways to model the impact of typhoon disasters on the transmission lines. The first one assumes that the failure probability of a transmission line is associated with the weather intensity in extreme weather events [36]. In this case, the fragility curve of the transmission lines is shown in Fig. 3. The second one considers the cumulative impacts of typhoon disasters on the transmission lines [15]. For the sake of simplicity, in our work, the failure probabilities of transmission lines caused by TD and WYF are only associated with wind speed at each tower and the midpoint of each line segment, respectively. Hence, the coordinates of these locations need to be determined in advance. Then, the wind speed at these locations in each specific typhoon disaster can be calculated through the motion path simulation and the wind field simulation.

Assume that the failures of lines are independent, the probability of line failure related to TD or WYF can be derived,

Authorized licensed use limited to: b-on: Universidade de Coimbra. Downloaded on November 09,2024 at 17:13:41 UTC from IEEE Xplore. Restrictions apply.

respectively [36].

$$p_{l,t}^{tower} = 1 - \prod_{i=1}^{I_l} (1 - p_{l,i}(v_{i,t})) \tag{14}$$

$$p_{l,t}^{flashover} = 1 - \prod_{j=1}^{J_l} (1 - p_{l,j}(v_{j,t})) \tag{15}$$

where $p_{l,t}^{tower}$ and $p_{l,t}^{flashover}$ represent the failure probability of line *l* caused by TD or WYF at timestamp *t*, respectively; I_l and J_l represent the number of towers and line segments of line *l*; $p_{l,i}$ and $p_{l,j}$ represent the failure probability of tower *i* and line segment *j* of line *l*, respectively; $v_{i,t}$ and $v_{j,t}$ describe the wind speed at tower *i* and the midpoint of line segment *j* at timestamp *t*, respectively.

C. Stochastic Optimization Model

1) Mathematical Formulation: The TDH problem with DDU is formulated as a two-stage SMIP. In the optimization model, only the impact of the typhoon disasters on the transmission lines is considered. The first stage is to make hardening decisions, and the second stage is to calculate the costs related to load shedding and repair tasks in the realized typhoon disaster scenarios. The overall formulation, including the linearization method, is presented as follows. The objective of the proposed two-stage SMIP is to minimize the expected costs, including the enhancement cost, repair cost, and penalty cost for load shedding with respect to the probability of each scenario, as shown in equation (16). Notably, the enhancement cost has been converted into the equivalence annual cost.

$$\min C^E + \omega \mathbb{E}_s \phi(s) \tag{16}$$

$$\text{s.t.} \quad \sum_{l \in L} x_l^{tower} + \sum_{l \in L} x_l^{flashover} \le N_L \tag{17}$$

$$\sum_{a \in A} x_l^{a,T} = x_l^{tower} \tag{18}$$

$$\sum_{b \in B} x_l^{b,F} = x_l^{flashover} \tag{19}$$

$$C^E = \sum_{l \in L, a \in A} c_l^a x_l^{a,T} + \sum_{l \in L, b \in B} c_l^b x_l^{b,F} \tag{20}$$

$$\text{where} \quad \mathbb{E}_s \phi(s) = \sum_S \pi^s \phi(s) \tag{21}$$

$$\text{with} \quad \phi(s) = \min C^{R,s} + C^{L,s} \tag{22}$$

$$\text{s.t.} \quad u_{l,t}^s = (1 - x_l^{tower}) \xi_{l,t}^{0,s} + \sum_{a \in A} x_l^{a,T} \xi_{l,t}^{a,s} \tag{23}$$

$$v_{l,t}^s = (1 - x_l^{flashover}) \gamma_{l,t}^{0,s} + \sum_{b \in B} x_l^{b,F} \gamma_{l,t}^{b,s} \tag{24}$$

$$y_{l,t}^s = \max(u_{l,t}^s, v_{l,t}^s) \tag{25}$$

$$0 \le P_{g,t}^s \le P_g^{\max} \tag{26}$$

$$0 \le \tilde{P}_{d,t}^s \le P_{d,t} \tag{27}$$

$$\theta_b^{\min} \le \theta_{b,t}^s \le \theta_b^{\max} \tag{28}$$

$$-(1 - y_{l,t}^s) P_l^{\max} \le P_{l,t}^s \le (1 - y_{l,t}^s) P_l^{\max} \tag{29}$$

$$-M_c y_{l,t}^s \le \left(\theta_{l,fr,t}^s - \theta_{l,to,t}^s\right) b_l - P_{l,t}^s \le M_c y_{l,t}^s \tag{30}$$

$$\sum_{g \in G_b} P_{g,t}^s - \sum_{l \in LF_b} P_{l,fr,t}^s + \sum_{l \in LT_b} P_{l,to,t}^s = \sum_{d \in D_b} \left(P_{d,t}^s - \tilde{P}_{d,t}^s\right) \tag{31}$$

$$C^{R,s} = c^R \cdot \sum_{l \in L} \sum_T y_{l,t}^s \tag{32}$$

$$C^{L,s} = c_d \sum_{d \in D_b} \sum_T \tilde{P}_{d,t}^s \tag{33}$$

Constraint (17) restricts the number of enhancement measures that can be taken. Constraint (18) indicates that there is a mutually exclusive relationship of enhancement measures against TD. Similarly, constraint (19) describes the relationship of enhancement measures against WYF. Namely, only one measure can be taken for the same target if a transmission line is selected for hardened. For instance, if there is a transmission line *l* to be hardened against TD, $x_l^{tower} = 1$, then one of $\{x_l^{a,T}, a \in A\}$is equal to 1 and the others are forced to be equal to 0. While $x_l^{tower} = 0$, all of $\{x_l^{a,T}, a \in A\}$will be forced to 0. The investment cost of hardening the transmission lines is given by equation (20).

The expectation of repair cost and penalty cost for load shedding derived by solving the second-stage problem is formulated as equation (21). With the fixed value of the first-stage decision variables and a specific scenario *s*, the second-stage problem can be described by (22)-(33). Equation (22) denotes the objective function of the second-stage problem. Constraints (23)–(24) represent the transmission line damage status caused by TD and WYF in a realized typhoon scenario, respectively. It will be introduced in detail in 2) *Decision-dependent Uncertainty Modeling*. Constraint (25) indicates that both TD and WYF can lead to transmission line outages.

Constraints (26)–(31) are the direct-current power flow constraints. Constraint (26) limits the output of the generation units. Constraint (27) limits the amount of load shedding. Constraint (28) limits the phase angle of the buses. Constraints (29)–(30) determine the power flow through each transmission line. When line *l* is in a power outage state, i.e., $y_{l,t}^s = 1$, there is no power flow on it. Otherwise, $P_{l,t}^s = (\theta_{l,fr,t}^s - \theta_{l,to,t}^s) b_l$ is satisfied. Constraint (31) ensures power balance on each bus. The repair cost and penalty cost for load shedding are given by equations (32) and (33), respectively.

Since constraint (25) is a non-linear constraint, the linearized method is required to apply to it as follows:

$$y_{l,t}^s \ge u_{l,t}^s \tag{34}$$

$$y_{l,t}^s \ge v_{l,t}^s \tag{35}$$

$$y_{l,t}^s \le u_{l,t}^s + M_c \left(1 - w_{l,t,1}^s\right) \tag{36}$$

$$y_{l,t}^s \le v_{l,t}^s + M_c \left(1 - w_{l,t,2}^s\right) \tag{37}$$

Authorized licensed use limited to: b-on: Universidade de Coimbra. Downloaded on November 09,2024 at 17:13:41 UTC from IEEE Xplore. Restrictions apply.

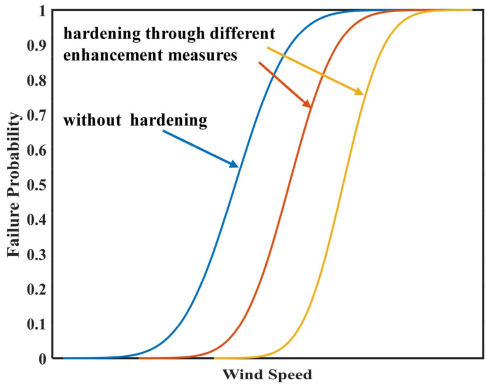

Fig. 4. Illustration of decision-dependent uncertainty.

$$w^s_{l,t,1} + w^s_{l,t,2} \geq 1 \tag{38}$$

2) Decision-Dependent Uncertainty Modeling: To explain the concept intuitively, the illustration of DDU related to whether the transmission line is hardened or not is presented in Fig. 4. The failure probability of a transmission line will decrease to varying degrees according to the different enhancement measures. Since the failure probability is associated with the hardening decision which is unknown before solving the optimization model, the decision-dependent failure probability is difficult to be described analytically. Hence, the specific line damage scenarios cannot be generated for solving the proposed optimization problem.

The modeling technique proposed in [21] is adopted to deal with the challenge in this work. In constraints (23)-(24), the auxiliary parameters are introduced to represent the status of transmission lines with or without hardening. For instance, assume that there are a total of three enhancement measures against TD, if measure 2 is taken on the transmission line 3, i.e., $x_3^{tower} = 1, x_3^{1,T} = 0, x_3^{2,T} = 1, x_3^{3,T} = 0$. Then, $u^s_{3,t} = \xi^{2,s}_{3,t}$ can be obtained. Then, the status of transmission line 3 (caused by TD) can be represented by the corresponding auxiliary parameter.

Note that the auxiliary parameters can be obtained independently in the phase of scenario generation. In this way, the model is formulated as a SMIP, with binary variables to select which set of expected costs is incurred in the second stage based on the enhancement measures available as a consequence of decisions in the first stage. The optimization model needs a large number of typhoon disaster scenarios to obtain a high-quality solution.

3) Scenario Generation: The procedure for scenario generation is as follows:

The procedure for scenario generation

1: Determine the coordinates of each tower and the midpoint of each line segment.
2: **for** scenario $s = 1, \ldots, |S|$ **do**
3: Determine the longitude and latitude of the landing place.
4: Sample $y_\theta, y_c, y_{\Delta p}$ from the uniform distribution U(0, 1).
5: Calculate $\theta(0), c(0), \Delta p(0)$ through equations (1)-(3).
6: Simulate the motion path using equations (4)-(7).
7: Simulate the wind field employing equations (8)-(13).
8: **for** timestamp $t = 1, \ldots, |T^s|$**do**
9: Calculate the distance between these locations and the center of the typhoon.
10: Obtain the wind speed at these locations via (8).
11: Calculate $p^{tower}_{l,t}$ and $p^{flashover}_{l,t}$ via (14) and (15).
12: Sample $\{p^a_1, a = 0, \ldots, |A|\}$ and$\{p^b_2, b = 0, \ldots, |B|\}$from the uniform distribution $U(0, 1)$.
13: $\xi^{a,s}_{l,t} = \begin{cases} 1, p^a_1 \leq p^{tower}_{l,t} or \xi^{a,s}_{l,t-1} = 1 \\ 0, otherwise \end{cases}$
14: $\gamma^{b,s}_{l,t} = \begin{cases} 1, p^b_2 \leq p^{flashover}_{l,t} or \gamma^{b,s}_{l,t-1} = 1 \\ 0, otherwise \end{cases}$
15: **end for**
16: **end for**

III. Solution Algorithm

In this section, the sample average approximation (SAA) algorithm is introduced to solve the proposed TDH problem under DDU. Firstly, a compact notation is utilized to express the proposed optimization model. Secondly, the reason for the SAA algorithm for solving the proposed model is discussed. Finally, the implementation steps of the SAA algorithm are presented in detail.

A. The Compact Notation of the Proposed Model

To discuss the proposed optimization model conveniently, it is presented in the form as follows:

$$\min_{\boldsymbol{x} \in \boldsymbol{X}} \boldsymbol{c}^T \boldsymbol{x} + \mathbb{E}_s \phi(\boldsymbol{x}, \boldsymbol{\zeta}) \tag{39}$$

$$\text{s.t.} \quad \boldsymbol{A}\boldsymbol{x} \leq \boldsymbol{b} \tag{40}$$

$$\boldsymbol{x} \in \{0, 1\} \tag{41}$$

$$\text{with} \quad \phi(\boldsymbol{x}, \boldsymbol{\zeta}) = \inf_{\boldsymbol{y}} \{\boldsymbol{q}^T \boldsymbol{y} : \boldsymbol{F}\boldsymbol{y} \leq \boldsymbol{H}(s) - \boldsymbol{G}(s)\boldsymbol{x}\} \tag{42}$$

where vector $\boldsymbol{x}$ represents the hardening decision in the first stage, vector $\boldsymbol{c}$ represents the enhancement cost coefficient and $\boldsymbol{\zeta} = (\boldsymbol{q}, \boldsymbol{F}, \boldsymbol{H}(s), \boldsymbol{G}(s))$ represents the vector of parameters in the second stage. The hardening decision $\boldsymbol{x}$ should be determined before a realization of $\boldsymbol{\zeta}$.

The problem has the following characteristics:

1) The formulation of the second stage problem $\mathbb{E}_s \phi(\boldsymbol{x}, \boldsymbol{\zeta})$ cannot be written in a closed form, and its value cannot be easily obtained.
2) The value of the function $\phi(\boldsymbol{x}, \boldsymbol{\zeta})$ is easily calculated for given $\boldsymbol{x}$ and $\boldsymbol{\zeta}$.
3) The feasible solution set $\boldsymbol{X}$, although finite, is too large to employ the enumeration approach.

B. Sample Average Approximation Algorithm

The characteristics mentioned above make the problem difficult to solve. A natural idea is to obtain a near-optimal

Authorized licensed use limited to: b-on: Universidade de Coimbra. Downloaded on November 09,2024 at 17:13:41 UTC from IEEE Xplore. Restrictions apply.

Algorithm 1: Sample Average Approximation.

1: Generate N^E scenarios of transmission line failures for evaluation.
2: **for** iteration $m = 1, \ldots, M$ **do**
3: Generate N scenarios of transmission line failures.
4: Solve the stochastic optimization problem $v_N^m = \min\{\boldsymbol{c}^T\boldsymbol{x} + \frac{1}{N}\sum_{n=1}^{N}\phi(\boldsymbol{x}, \zeta^n) : \boldsymbol{A}\boldsymbol{x} \leq \boldsymbol{b}\}$ and obtain $\boldsymbol{x}_N^m$.
5: Evaluate the solution x_N^m over N^E scenarios: $\mu_{N^E}^m = \frac{1}{N^E}\sum_{n=1}^{N^E}(\boldsymbol{c}^{\mathrm{T}}\boldsymbol{x}_N^m + \phi(\boldsymbol{x}_N^m, \zeta^n))$
6: **end for**
7: Select $\mu_U = \min_{m\in\{1,\ldots,M\}} \mu_{N^E}^m$ as the upper bound estimate, and obtain the corresponding near-optimal solution $\boldsymbol{x}^*$.
8: Calculate the variance of the upper bound estimate: $\sigma_U^2 = \frac{1}{N^E-1}\sum_{n=1}^{N^E}\left((\boldsymbol{c}^{\mathrm{T}}\boldsymbol{x}^* + \phi(\boldsymbol{x}^*, \zeta^n)) - \mu_U\right)^2$.
9: The $(1-\alpha)$ level confidence interval for the upper bound is constructed as $\mu_U \pm z_{\alpha/2}\sigma_U/\sqrt{N^E}$.
10: Calculate the lower bound estimate and its variance as $\mu_L = \frac{1}{M}\sum_{m=1}^{M} v_N^m$ and $\sigma_L^2 = \frac{1}{M-1}\sum_{m=1}^{M}(v_N^m - \mu_L)^2$.
11: The $(1-\alpha)$ level confidence interval for the lower bound is constructed as $\mu_L \pm t_{\alpha/2,M-1}\sigma_L/\sqrt{M}$.

solution and assess its quality. Consequently, the SAA algorithm is utilized to optimize the proposed model. The basic concept of SAA is easy to follow, i.e., the expected value function is approximated through the corresponding average function of random sample scenarios. Moreover, the CI of the optimal value can be obtained through the SAA algorithm.

Algorithm 1 outlines the key steps of the SAA algorithm [31]. Firstly, *M* batches of *N* scenarios of transmission line failures are generated. The stochastic optimization problems with *N* scenarios are solved, and the mean value of their objectives is utilized as a lower bound estimate of the optimal value. Then, the resulting *M* near-optimal solutions are evaluated over N^E scenarios where $N^E >> N$. The smallest one is selected as the upper bound estimate of the optimal value. Finally, the CI of the optimal value can be constructed as follows:

$$(\mu_L - t_{\alpha/2,M-1}\sigma_L/\sqrt{M}, \mu_U + z_{\alpha/2}\sigma_U/\sqrt{N^E}) \tag{43}$$

Note that three adjustable parameters, i.e., the number of evaluation scenarios N^E, the number of iterations *M*, and the number of optimization scenarios *N*, will affect the calculation results. These parameters can be adjusted to trade-off computational effort with the desired CI.

IV. Case Study

In this section, the numerical experiments are conducted on the modified IEEE RTS-79 system and the modified IEEE 118-Bus system to verify the effectiveness of the proposed framework. Mathematical models are established with YALMIP [37] and solved with Gurobi solver in MATLAB. The experiments are implemented on a workstation consisting of two 3.0 GHz 24-Core Intel Xeon Gold 6248R CPUs and 256 GB of RAM.

TABLE I
The Characteristic Parameters of the Probability Distribution Models

Parameter	Value	Parameter	Value
μ_θ	1.4590	σ_1	0.9388
σ_2	0.6015	$\mu_{\ln c}$	1.7788
$\sigma_{\ln c}$	0.2635	κ	4.179
χ	60.7977		

TABLE II
The Investment Cost Data of Enhancement Measures

Measure NO.	Objective	Effect	Enhancement Cost ($/tower or segment)
M1	TD	$\mathcal{N}$(39m/s, 0.5m/s)	500
M2	TD	$\mathcal{N}$(41m/s, 0.5m/s)	750
M3	WYF	$\mathcal{N}$(37m/s, 2.0m/s)	300
M4	WYF	$\mathcal{N}$(39m/s, 1.2m/s)	375
M5	WYF	$\mathcal{N}$(41m/s, 0.8m/s)	500

A. Data Description

The characteristic parameters describing the probability distribution of the typhoon landing parameters can be obtained by analyzing historical statistics of western Pacific typhoons that landed in Fujian, Guangdong, and Hong Kong, China from 1998 to 2010 [38], as listed in Table I.

Besides, the following assumptions are made in the numerical experiment due to lack of relevant statistics:

1) The wind speeds causing TD and WYF (without hardening) obey the normal distribution $\mathcal{N}(37\ \mathrm{m/s}, 0.5\ \mathrm{m/s})$ and $\mathcal{N}(35\ \mathrm{m/s}, 3\ \mathrm{m/s})$, respectively.
2) The effects and enhancement costs of enhancement measures are presented in Table II.
3) The penalty costs for load shedding and repair are set as 500 $/MW [39] and 25000 $/line, respectively.

Finally, repair tasks will only be carried out after the typhoon leaves. The total repair time is assumed as 24 hours. Therefore, if load shedding occurs, it will continue for 24 hours after the typhoon leaves.

B. Modified IEEE RTS-79 System

The modified IEEE RTS-79 system is utilized as the test system. Since summer is the season with a high incidence of typhoons, the load data of the 28th week is selected. The rated capacities of lines 25, 26, and 27 are modified to 0.35 p.u. The capacities of the remaining branches are limited to 0.6 p.u [40]. As typhoons often hit China's southeast coastal area, the test system is attached to the map of the area. The diagram of the test system is presented in Fig. 5. Additionally, four locations are selected as the typhoon landing sites with equal probability, and they are marked on the map in different colors. The typical

Authorized licensed use limited to: b-on: Universidade de Coimbra. Downloaded on November 09,2024 at 17:13:41 UTC from IEEE Xplore. Restrictions apply.

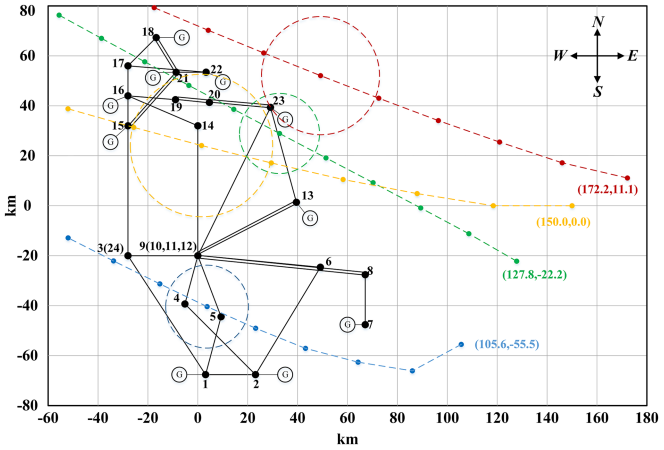

Fig. 5. The diagram of the modified IEEE RTS-79 system and the typical simulated typhoon motion path.

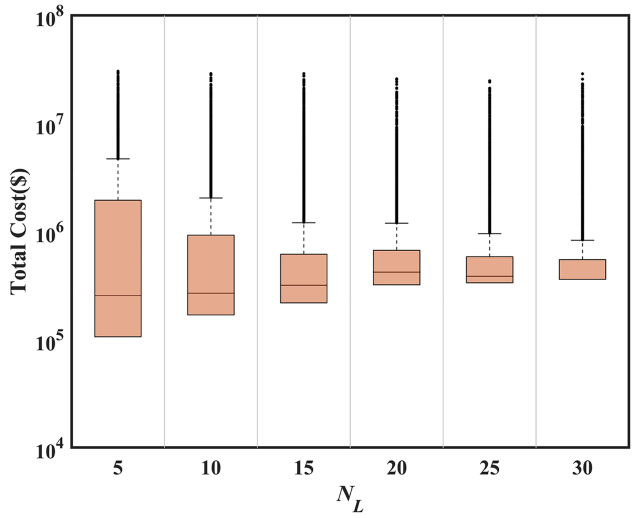

Fig. 6. The box plot of the evaluation values with different N_L.

TABLE III
RELEVANT COST CALCULATION RESULTS OF FIVE CASES

Case No.	Cost($\times 10^5$\$)		
	Enhancement	Repair	Load Shedding
1	0	2.949	29.356
2	0.085	2.947	29.209
3	2.302	1.335	8.535
4	4.014	1.217	2.667
5	6.683	1.032	1.114

typhoon motion path from each landing site is also shown in Fig. 5.

1) Calculation Results: To investigate the effectiveness of the proposed framework, four cases are considered.

Case 1: Without hardening the original system.
Case 2: Only line hardening against TD is permitted.
Case 3: Only line hardening against WYF is permitted.
Case 4: Both line hardening against TD and line hardening against WYF are permitted.
Case 5: Determine the hardening decisions using tri-level DAD robust optimization [5].

To make the result of Case 5 comparable with that of other cases, both M2 and M5 are implemented on the selected lines to as much as possible meet the assumption of the DAD framework that the hardened lines are invulnerable. Additionally, the same as other cases, the hardening decision of Case 5 is assessed through all evaluation scenarios to obtain expected costs. The relevant expected cost calculation results of five cases are presented in Table III.

It can be found that the repair cost and the penalty cost for load shedding decrease as the enhancement cost increases. In Case 2, only one transmission line is hardened. Therefore, the repair cost and the penalty cost for load shedding are just slightly reduced. This is because the wind speed that causes TD usually also causes WYF. If only line hardening against TD is permitted, there is still a high probability that the hardened lines will fail due to WYF. Consequently, it is not effective to just hardened transmission lines against TD. In contrast, although only line hardening against WYF is permitted in Case 3, it effectively reduces the repair cost and the penalty cost for load shedding.

Besides, what stands out in Table III is that the penalty costs for load shedding are reduced by 90.92% in Case 4 and 96.21% in Case 5, respectively. Besides, the repair costs also decrease significantly in these two cases. It can be inferred that hardening transmission lines against TD and WYF at the same time can maximize the system's ability to withstand extreme weather. However, the hardening decision of Case 5 is obtained without simulating typhoon disasters and considering the worst situation. Whether the transmission line is hardened or not, depends on its importance to the system. Hence, some transmission lines that are not easily influenced by typhoon disasters are also hardened. Although the repair cost and penalty cost for load shedding in Case 5 are lower than those in Case 4, the enhancement cost is significantly higher than that in Case 4, resulting in a total expected cost that is 11.79% higher than that in Case 4. It indicates the importance of modeling the uncertainty of extreme weather events in pre-disaster defense planning. Additionally, the hardening decision of Case 4 is not a simple combination of Case 2 and Case 3. The result fully demonstrates the effectiveness of the proposed optimization model.

Finally, note that the hardened components also can be influenced by weather events. Namely, the transmission line may still be damaged by the typhoon after enhancement which is practical in engineering applications. Nevertheless, TDH still shows a positive effect in preventing power outages in extreme weather.

2) Analysis of the Number of Enhancement Measures Taken: To investigate the trend of the total cost with the number of enhancement measures taken, we conduct the numerical experiments with $N_L = 5, 10, 15, 20, 25, 30$. In addition, the other parameters are set as $N^E = 10000$, $M = 10$, $N = 200$.

Fig. 6 represents the box plot of the evaluation values of near-optimal solution over N^E scenarios with different values of N_L. It can be observed that there are some outliers in each

Authorized licensed use limited to: b-on: Universidade de Coimbra. Downloaded on November 09,2024 at 17:13:41 UTC from IEEE Xplore. Restrictions apply.

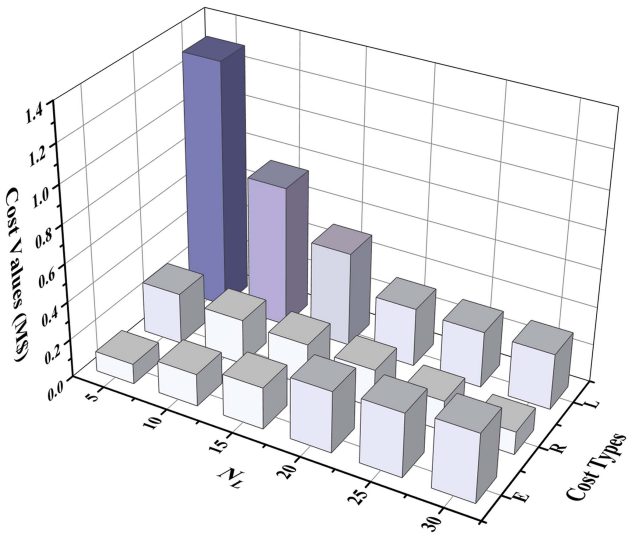

Fig. 7. The relevant costs with different N_L.

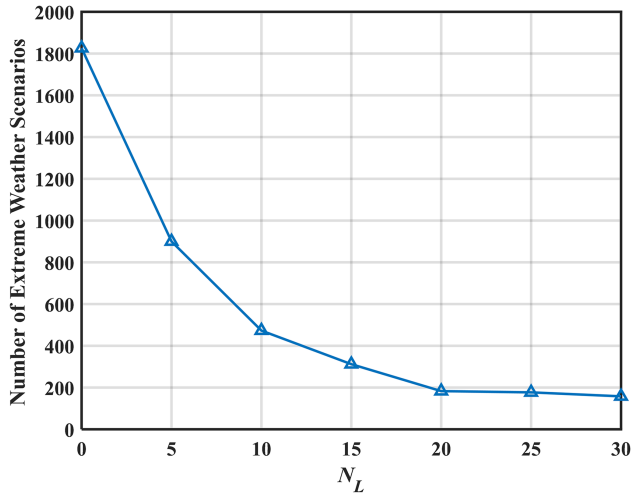

Fig. 8. The number of extreme weather scenarios with different N_L.

case. This is because TDH cannot guarantee that the test system can completely withstand typhoon disasters. Many transmission lines will still be damaged, causing blackouts, leading to a high penalty cost for load shedding in some extreme typhoon disasters. Besides, it can be seen that the height of the box decreases as the value of N_L grows. On the one hand, the investment cost increases with the value of N_L, leading to the bottom of the box rising. On the other hand, the reduction in penalty cost for load shedding makes the top of the box drop. This phenomenon reflects the role of TDH in that it reduces the risk of certain typhoon disasters to the power system at the expense of increased enhancement costs. Additionally, note that the bottom of the box represents the enhancement cost. It can be inferred that more than 50% of typhoon scenarios will not cause severe damage to the system with $N_L = 30$.

Fig. 7 illustrates the relevant costs with different N_L, where 'E' means enhancement cost, 'R' means repair cost, and 'L' means penalty cost for load shedding. It is observed from Fig. 7 that the repair cost and penalty cost for load shedding are gradually declined as N_L is increased. The penalty cost for load shedding accounts for the most significant proportion of total cost when N_L is small. When N_L reaches 20, the enhancement cost contributes the most to the total cost. We define the critical cost value of extreme weather scenarios as 6 M$, which is approximately twice the expected cost of an unhardened system. Fig. 8 presents the number of extreme weather scenarios with different N_L. The downward trend of extreme weather scenarios is similar to that of penalty cost for load shedding. The number of extreme weather scenarios decreases significantly with the increase of N_L when N_L is small, and when N_L reaches 20, it decreases slowly as N_L grows. Figs. 7 and 8 together prove the importance of TDH for an under-hardened system.

Generally, if a transmission line is hardened against TD and WYF at the same time in the enhancement plan, it can be inferred that this line is relatively critical. Table IV shows the critical lines in the resilience enhancement portfolios in each case. It can be found that line 7–8 appears in every case. Line 7–8 is the line closest to the coastline. Therefore, it is easier to be destroyed in typhoon disasters. Moreover, there are three 100 MW generation units connected to bus 7. But line 7–8 is the only line that can deliver the energy generated by these generation units outward. Once it is damaged, it will affect the active power supply of the system. Consequently, it is selected as the critical component for hardening due to its fragility and importance to the system. Additionally, lines 12–23, 14–16, and 20–23 are also critical components that need to be hardened. They are vulnerable to typhoon disasters due to their geographical location since typhoons in this area usually move from southeast to northwest.

TABLE IV
RELATIVE CRITICAL LINES IN THE ENHANCEMENT PORTFOLIOS

N_L	Transmission Lines
5	7-8,12-23
10	7-8,12-23,14-16,20-23
15	7-8,12-23,14-16,16-19,20-23
20	1-5,7-8,11-14,12-23,14-16,15-24,19-20,20-23
25	2-6,7-8,11-13,13-23,14-16,15-24,16-19,19-20
30	2-6,4-9,7-8,12-23,14-16,19-20,20-23

TABLE V
RELEVANT EXPECTED COST CALCULATION RESULTS OF THREE SITUATIONS

Situation No.	Cost($\times 10^5$\$)		
	Enhancement	Repair	Load Shedding
1	4.014	1.217	2.667
2	2.929	1.107	3.106
3	4.747	1.380	2.959

3) Sensitive Analysis: Since the transmission line failure probability distributions are assumed, it is necessary to explore the effect of different failure probability distributions on the hardening decisions. The following three situations are considered. The relevant expected cost calculation results of three situations are presented in Table V.

Situation 1: The originally assumed failure probability distributions.

Authorized licensed use limited to: b-on: Universidade de Coimbra. Downloaded on November 09,2024 at 17:13:41 UTC from IEEE Xplore. Restrictions apply.

TABLE VI
THE STATISTICAL GAP FOR DIFFERENT NUMBER OF OPTIMIZATION SCENARIOS

N	CI for lower bound ($\times 10^6$\$)	CI for upper bound ($\times 10^6$\$)	Gap
100	(6.3414,6.6253)	(8.1584,8.1645)	22.34%
150	(6.7857,7.2348)	(7.9419,7.9475)	14.62%
200	(7.3862,7.9023)	(7.8941,7.9001)	6.51%
250	(6.8800,7.3898)	(7.6264,7.6320)	9.86%
300	(7.4360,7.6965)	(7.5915,7.5971)	2.12%

TABLE VII
THE STATISTICAL GAP FOR DIFFERENT NUMBER OF EVALUATION SCENARIOS

N^E	CI for lower bound ($\times 10^6$\$)	CI for upper bound ($\times 10^6$\$)	Gap
2000	(7.3862,7.9023)	(8.2886,8.3199)	11.24%
4000	(7.3862,7.9023)	(8.1303,8.1461)	9.34%
6000	(7.3862,7.9023)	(8.1883,8.1988)	9.92%
8000	(7.3862,7.9023)	(7.9605,7.9680)	7.31%
10000	(7.3862,7.9023)	(7.8941,7.9001)	6.51%

TABLE VIII
THE STATISTICAL GAP FOR DIFFERENT NUMBER OF ITERATIONS

M	CI for lower bound ($\times 10^5$\$)	CI for upper bound ($\times 10^5$\$)	Gap
5	(7.1721,8.6297)	(8.5804,8.5877)	16.49%
10	(7.3862,7.9023)	(7.8941,7.9001)	6.51%
15	(7.4714,7.6978)	(7.6942,7.7002)	2.97%
20	(7.4174,7.6091)	(7.6545,7.6601)	3.17%

Situation 2: The wind speeds causing TD and WYF (without hardening) obey the normal distribution $\mathcal{N}(38\ \mathrm{m/s}, 0.5\ \mathrm{m/s})$ and $\mathcal{N}(36\ \mathrm{m/s}, 3\ \mathrm{m/s})$, respectively.

Situation 3: The wind speeds causing TD and WYF (without hardening) obey the normal distribution $\mathcal{N}(36\ \mathrm{m/s}, 0.5\ \mathrm{m/s})$ and $\mathcal{N}(34\ \mathrm{m/s}, 3\ \mathrm{m/s})$, respectively.

The results indicate that Situation 2 has the lowest expected cost, followed by Situation 1, and Situation 3 with the highest expected cost. It is highly correlated with the robustness of the system. The wind resistance of the transmission lines significantly affects the hardening decision-making, resulting in the difference in enhancement cost being the largest among these three costs. Therefore, accurately assessing the wind resistance of each transmission line is a critical step in the TDH problem.

4) Computational Performance of SAA Algorithm: According to Algorithm 1, there are three parameters, including the number of optimization scenarios *N*, the number of evaluation scenarios N^E, and the number of iterations *M* can affect the confidence level of the result. The solution to the proposed problem tends to be better as *N* increases, and the optimal solution can be achieved when *N* is infinite. The number of evaluation scenarios N^E mainly affects the upper bound estimate. The number of iterations *M* will affect the lower bound estimate. Meanwhile, it also affects the probability that the SAA algorithm finds the optimal solution. In this section, we will explore the effect of these three parameters on the optimality gap. Note that the optimality gap is a statistical gap that can be used to roughly quantify the quality of the obtained solution. The results are presented in Tables VI to VIII. The situation where $N = 200$, $N^E = 10000$, and $M = 10$ is selected as the benchmark.

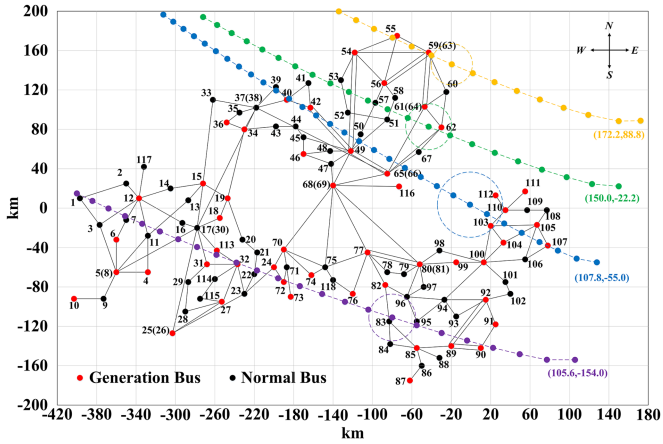

Fig. 9. The diagram of the modified IEEE 118-bus system and the typical simulated typhoon motion path.

As shown in Tables VI to VIII, the statistical optimality gap generally decreases with the increase of the respective parameter values. However, the computational complexity for solving the SAA problem increase usually exponentially as *N* grows. Similarly, the computation effort is also highly related to the values of N^E and *M*. Therefore, these parameters may need to be adjusted to trade-off computation time with the desired confidence level. Note that the parallel technique can be used to speed up the evaluation in Step 5. Additionally, our numerical experiments suggest that the parameter setting in the benchmark provides a relatively accurate solution within a reasonable time for solving the TDH problem.

C. Modified IEEE 118-Bus System

The modified IEEE 118-bus system is utilized as another test system. It includes 54 generators and 177 transmission lines. Similarly, the diagram of the test system is presented in Fig. 9. Four locations are selected as the typhoon landing sites with equal probability, and they are marked on the map in different colors. The typical typhoon motion path from each landing site is also shown in Fig. 9.

The proposed framework still shows good results on the modified IEEE 118-Bus system. The expected cost of the initial system is 1.927×10^6\$, including 4.520×10^5\$ in repair cost, and 1.475×10^6\$ in penalty cost for load shedding. After hardening, the expected cost is reduced significantly by 38.27% to 1.1895×10^6\$, including 4.552×10^5\$ in enhancement cost, 3.403×10^5\$ in repair cost, and 3.940×10^5\$ in penalty cost for load shedding.

There are a total of 49 enhancement measures that should be implemented, 10 of which are implemented on the lines further from the coastline. Specifically, the abscissas of the endpoints of these lines are less than -140km. Besides, the lines that need to strengthen the towers are concentrated in the southeast of the map near the coastline. This is because typhoons usually have high speeds when they make landfall, and then drop in wind speed as they move inland, resulting in significant differences in

Authorized licensed use limited to: b-on: Universidade de Coimbra. Downloaded on November 09,2024 at 17:13:41 UTC from IEEE Xplore. Restrictions apply.

individual failure probabilities related to typhoon disasters. Consequently, it is necessary to accurately simulate typhoon disaster scenarios to differentiate the individual failure probabilities.

V. Conclusion and Future Work

A. Conclusion

This paper presents a comprehensive optimization framework for solving the TDH under DDU against typhoon disasters. First, we leverage Monte Carlo-based sampling to simulate each typhoon disaster's motion path and wind field through the empirical track model and Batts model. A modeling strategy is introduced to decouple the interdependency between first-stage hardening decisions and line damage status. Then, the sampled scenarios are integrated into the proposed SMIP model. Finally, we solve the proposed SMIP model with a statistical sampling approach called the SAA algorithm. This algorithm enables determining the near-optimal resilience enhancement portfolio and obtaining the CI for the total cost.

The numerical experiments are conducted on the modified IEEE RTS-79 system and the modified IEEE 118-Bus system, respectively. The results demonstrate that the proposed framework provides noteworthy improvements over the models that only harden transmission lines against TD or WYF. Compared with the classical DAD framework, it indicates the importance of modeling the uncertainty of typhoon disasters and considering enhancement measures for different failures, in TDH. Besides, the result shows the superior performance of TDH in reducing power outages in extreme typhoon disasters and remarkable expected cost savings of up to 75.56% annually in the modified IEEE RTS-79 system. Finally, our analysis reveals the significance of TDH for an under-hardened system. Notably, the proposed framework can be modified to deal with other natural disasters.

B. Future Works

In the future, we would like to refine the proposed framework by exploring some factors that exist but are not considered. For example, the substation and generation unit failure probabilities related to typhoon disasters, other enhancement measures like the expansion to boost power system resilience, the joint failure probability of dependent line, etc.

Additionally, a relatively robust system will still be threatened by extreme typhoon disasters. It may not be a wise choice to continue to harden the system. Therefore, we would like to explore other ways to improve system resistance to risk in the future. For example, catastrophe insurance, resilience-oriented response, and resilience-oriented restoration are some effective supplementary means.

Acknowledgment

The authors would like to thank the China Scholarship Council for funding Weixin Zhang's research in Italy.

References

[1] "Hurricane FAQ – NOAA's Atlantic oceanographic and meteorological laboratory," Accessed: May 11, 2022. [Online]. Available: https://www.aoml.noaa.gov/hrd-faq/

[2] E. S. Blake, T. B. Kimberlain, R. J. Berg, J. P. Cangialosi, and J. L. Beven II, "Tropical cyclone report hurricane sandy (AL182012) 22-29 October 2012," National Hurricane Center, Feb. 2013.

[3] "Typhoon 'Meranti' caused a direct economic loss of 21.073 billion RMB in fujian and zhejiang," Accessed: Mar. 28, 2022. [Online]. Available: http://news.cctv.com/2016/09/18/ARTIk6Zo5QUUQ2Mt5fLektiU160918.shtml

[4] H. Hamidpour, S. Pirouzi, S. Safaee, M. Norouzi, and M. Lehtonen, "Multi-objective resilient-constrained generation and transmission expansion planning against natural disasters," *Int. J. Elect. Power Energy Syst.*, vol. 132, Nov. 2021, Art. no. 107193.

[5] A. Bagheri, C. Zhao, F. Qiu, and J. Wang, "Resilient transmission hardening planning in a high renewable penetration era," *IEEE Trans. Power Syst.*, vol. 34, no. 2, pp. 873–882, Mar. 2019.

[6] M. Panteli, D. N. Trakas, P. Mancarella, and N. D. Hatziargyriou, "Power systems resilience assessment: Hardening and smart operational enhancement strategies," *Proc. IEEE*, vol. 105, no. 7, pp. 1202–1213, Jul. 2017.

[7] G. Brown, M. Carlyle, J. Salmerón, and K. Wood, "Analyzing the vulnerability of critical infrastructure to attack and planning defenses," in *Tuts. Operat. Res.: Emerg. Theory, Methods, Appl.*, 2005, pp. 102–123.

[8] W. Yuan, L. Zhao, and B. Zeng, "Optimal power grid protection through a defender–attacker–defender model," *Rel. Eng. System Saf.*, vol. 121, pp. 83–89, Jan. 2014.

[9] Y. Fang and G. Sansavini, "Optimizing power system investments and resilience against attacks," *Rel. Eng. System Saf.*, vol. 159, pp. 161–173, Mar. 2017.

[10] W. Yuan, J. Wang, F. Qiu, C. Chen, C. Kang, and B. Zeng, "Robust optimization-based resilient distribution network planning against natural disasters," *IEEE Trans. Smart Grid*, vol. 7, no. 6, pp. 2817–2826, Nov. 2016.

[11] J. Yan, B. Hu, K. Xie, J. Tang, and H.-M. Tai, "Data-Driven transmission defense planning against extreme weather events," *IEEE Trans. Smart Grid*, vol. 11, no. 3, pp. 2257–2270, May 2020.

[12] S. Ma, B. Chen, and Z. Wang, "Resilience enhancement strategy for distribution systems under extreme weather events," *IEEE Trans. Smart Grid*, vol. 9, no. 2, pp. 1442–1451, Mar. 2018.

[13] M. Panteli and P. Mancarella, "Modeling and evaluating the resilience of critical electrical power infrastructure to extreme weather events," *IEEE Syst. J.*, vol. 11, no. 3, pp. 1733–1742, Sep. 2017.

[14] R. Rocchetta, E. Zio, and E. Patelli, "A power-flow emulator approach for resilience assessment of repairable power grids subject to weather-induced failures and data deficiency," *Appl. Energy*, vol. 210, pp. 339–350, Jan. 2018, doi: 10.1016/j.apenergy.2017.10.126.

[15] X. Liu et al., "A planning-oriented resilience assessment framework for transmission systems under typhoon disasters," *IEEE Trans. Smart Grid*, vol. 11, no. 6, pp. 5431–5441, Nov. 2020.

[16] T. Kanungo, D. M. Mount, N. S. Netanyahu, C. D. Piatko, R. Silverman, and A. Y. Wu, "An efficient k-means clustering algorithm: Analysis and implementation," *IEEE Trans. Pattern Anal. Mach. Intell.*, vol. 24, no. 7, pp. 881–892, Jul. 2002.

[17] H. Heitsch and W. Römisch, "Scenario reduction algorithms in stochastic programming," *Comput. Optim. Appl.*, vol. 24, no. 2, pp. 187–206, Feb. 2003.

[18] N. R. Romero, L. K. Nozick, I. D. Dobson, N. Xu, and D. A. Jones, "Transmission and generation expansion to mitigate seismic risk," *IEEE Trans. Power Syst.*, vol. 28, no. 4, pp. 3692–3701, Nov. 2013.

[19] M. Movahednia, A. Kargarian, C. E. Ozdemir, and S. C. Hagen, "Power grid resilience enhancement via protecting electrical substations against flood hazards: A stochastic framework," *IEEE Trans. Ind. Inform.*, vol. 18, no. 3, pp. 2132–2143, Mar. 2022.

[20] M. Bynum et al., "Proactive operations and investment planning via stochastic optimization to enhance power systems' extreme weather resilience," *J. Infrastructure Syst.*, vol. 27, no. 2, Jun. 2021, Art. no. 04021004.

[21] S. Ma, L. Su, Z. Wang, F. Qiu, and G. Guo, "Resilience enhancement of distribution grids against extreme weather events," *IEEE Trans. Power Syst.*, vol. 33, no. 5, pp. 4842–4853, Sep. 2018.

[22] L. Hellemo, P. I. Barton, and A. Tomasgard, "Decision-dependent probabilities in stochastic programs with recourse," *Comput. Manag. Sci.*, vol. 15, no. 3/4, pp. 369–395, Oct. 2018.

Authorized licensed use limited to: b-on: Universidade de Coimbra. Downloaded on November 09,2024 at 17:13:41 UTC from IEEE Xplore. Restrictions apply.

[23] State Grid Typhoon Monitoring & Warning Center, "Characteristics of typhoon disasters on high-voltage overhead transmission lines and their application in early warning," Accessed: Mar. 17, 2022. [Online]. Available: https://www.doc88.com/p-21461720481853.html
[24] F. Albermani, M. Mahendran, and S. Kitipornchai, "Upgrading of transmission towers using a diaphragm bracing system," *Eng. Structures*, vol. 26, no. 6, pp. 735–744, May 2004.
[25] C. Lu, X. Ma, and J. E. Mills, "The structural effect of bolted splices on retrofitted transmission tower angle members," *J. Constructional Steel Res.*, vol. 95, pp. 263–278, Apr. 2014.
[26] *Technical Specification for Windproof Design of Transmission Lines of China Southern Power Grid*, China Southern Power Grid Standard Q/CSG-2016, 2016.
[27] P. J. Vickery, P. F. Skerlj, and L. A. Twisdale, "Simulation of hurricane risk in the U.S. using empirical track model," *J. Struct. Eng.*, vol. 126, no. 10, pp. 1222–1237, Oct. 2000.
[28] M. E. Batts, E. Simiu, and L. R. Russell, "Hurricane wind speeds in the United States," *J. Struct. Division*, vol. 106, no. 10, pp. 2001–2016, Oct. 1980.
[29] A. J. Kleywegt, A. Shapiro, and T. Homem-de-Mello, "The sample average approximation method for stochastic discrete optimization," *SIAM J. Optim.*, vol. 12, no. 2, pp. 479–502, Jan. 2002.
[30] S. Ahmed and A. Shapiro, "The sample average approximation method for stochastic programs with integer recourse," ISyE Technical Report, Georgia Inst. Technol., pp. 1–24, 2002.
[31] B. Basciftci, S. Ahmed, N. Z. Gebraeel, and M. Yildirim, "Stochastic optimization of maintenance and operations schedules under unexpected failures," *IEEE Trans. Power Syst.*, vol. 33, no. 6, pp. 6755–6765, Nov. 2018.
[32] J. Kaplan and M. DeMaria, "A simple empirical model for predicting the decay of tropical cyclone winds after landfall," *J. Appl. Meteorol. Climatol.*, vol. 34, no. 11, pp. 2499–2512, Nov. 1995.
[33] Z. Toth and T. Szentimrey, "The binormal distribution: A distribution for representing asymmetrical but Normal-like weather elements," *J. Climate*, vol. 3, no. 1, pp. 128–136, Jan. 1990.
[34] P. N. Georgiou, A. G. Davenport, and B. J. Vickery, "Design wind speeds in regions dominated by tropical cyclones," *J. Wind Eng. Ind. Aerodynamics*, vol. 13, no. 1, pp. 139–152, Dec. 1983.
[35] P. J. Vickery and L. A. Twisdale, "Prediction of hurricane wind speeds in the United States," *J. Struct. Eng.*, vol. 121, no. 11, pp. 1691–1699, Nov. 1995.
[36] M. Panteli, D. N. Trakas, P. Mancarella, and N. D. Hatziargyriou, "Boosting the power grid resilience to extreme weather events using defensive islanding," *IEEE Trans. Smart Grid*, vol. 7, no. 6, pp. 2913–2922, Nov. 2016.
[37] J. Lofberg, "YALMIP : A toolbox for modeling and optimization in MATLAB," in *Proc. IEEE Int. Conf. Robot. Automat. (IEEE Cat. No.04CH37508)*, 2004, pp. 284–289.
[38] "Typhoon Motion Path," Accessed: Apr. 18, 2022. [Online]. Available: https://typhoon.slt.zj.gov.cn/default.aspx
[39] E. Du, N. Zhang, C. Kang, and Q. Xia, "Scenario map based stochastic unit commitment," *IEEE Trans. Power Syst.*, vol. 33, no. 5, pp. 4694–4705, Sep. 2018.
[40] W. Zhang et al., "Short-Term transmission maintenance scheduling considering network topology optimization," *J. Modern Power Syst. Clean Energy*, vol. 10, no. 4, pp. 883–893, Jul. 2022.

Weixin Zhang received the B.S. degree in 2018 from Chongqing University, Chongqling, China, where he is currently working toward the Ph.D. degree. He is also a Visiting Ph.D. Student with the University of Salerno, Salerno, Italy. His research interests include power system risk assessment and optimization.

Changzheng Shao (Member, IEEE) received the B.S. degree in electrical engineering from Shandong University, Jinan, China, in 2015, and the Ph.D. degree from Zhejiang University, Hangzhou, China, in 2020. He is currently an Assistant Professor with Chongqing University, Chongqong, China. His research interests include the operation optimization and reliability evaluation of the integrated energy system.

Bo Hu (Member, IEEE) received the Ph.D. degree in electrical engineering from Chongqing University, Chongqong, China, in 2010. He is currently a Full Professor with the School of Electrical Engineering. His research interests include power system reliability and parallel computing techniques in power systems. He is also the Editor of the IEEE TRANSACTIONS ON POWER SYSTEMS.

Kaigui Xie (Senior Member, IEEE) received the Ph.D. degree in power system and its automation from Chongqing University, Chongqong, China, in 2001. He is currently a Full Professor with the School of Electrical Engineering, ChongQing University. He has authored or coauthored more than 200 academic papers and five books. His main research interests include power system reliability, planning, and analysis. Prof. Xie was the Editor of the IEEE TRANSACTIONS ON POWER SYSTEMS.

Pierluigi Siano (Senior Member, IEEE) received the M.Sc. degree in electronic engineering and the Ph.D. degree in information and electrical engineering from the University of Salerno, Salerno, Italy, in 2001 and 2006, respectively. He is currently a Professor and Scientific Director of the Smart Grids and Smart Cities Laboratory, Department of Management and Innovation Systems, University of Salerno. Since 2021, he has been a Distinguished Visiting Professor with the Department of Electrical and Electronic Engineering Science, University of Johannesburg, Johannesburg, South Africa. He has coauthored more than 680 articles, including more than 410 international journals that received in Scopus more than 15240 citations with an H-index equal to 61 in his research areas, which include centered on demand response, energy management, the integration of distributed energy resources in smart grids, electricity markets, and planning and management of power systems. In 2019, 2020, and 2021, he was awarded as a Highly Cited Researcher in Engineering by Web of Science Group. He is the Chair of the IES TC on Smart Grids. He is also the Editor of the Power & Energy Society Section of IEEE ACCESS, IEEE TRANSACTIONS ON POWER SYSTEMS, IEEE TRANSACTIONS ON INDUSTRIAL INFORMATICS, IEEE TRANSACTIONS ON INDUSTRIAL ELECTRONICS, and IEEE SYSTEMS.

Mushui Li received the M.S. degree from the Chongqing University, Chongqing, China, in 2020. He is currently an Employee of State Grid Chongqington Changshou Electric Power Supply Branch, China.

Maosen Cao received the B.S. degree in electrical engineering from Southwest Jiaotong University, Chengdu, China, in 2018. He is currently working toward the Ph.D. degree with Chongqing University, Chongqong, China. His research interests include reliability assessment and optimization of the integrated energy system.

Authorized licensed use limited to: b-on: Universidade de Coimbra. Downloaded on November 09,2024 at 17:13:41 UTC from IEEE Xplore. Restrictions apply.